A Multi-Harmonic Probe Technique for Computing Oscillator Steady States

Kapil Dev Boianapally, Ting Mei and Jaijeet Roychowdhury
ECE Department, University of Minnesota, Minneapolis, MN, USA

Abstract— **We present a novel method for finding periodic steady states of general classes of oscillators robustly. The new method, which we term the *multi-harmonic probe (MHP) technique*, generalizes the well-known technique of augmenting harmonic balance (HB) for oscillators using an external probe. By using non-sinusoidal periodic probes, MHP enhances the applicability of the standard probe method (which uses purely sinusoidal probes) to broader classes of oscillators. We thus obtain a general and robust method for the periodic steady state of any kind of oscillator. Results on LC and ring oscillator circuits are presented that testify to the efficacy of our approach.**

I. Introduction

Oscillators are circuits which generate periodic, time-varying waveforms from only DC inputs. They are essential components in many electronic circuits; finding application, for example, as local oscillators for up/down-conversion in communication systems, clocks that provide timing signals in digital circuits, within PLLs, and in clock/data recovery circuits. Despite being very widely used, finding the periodic steady state of oscillators still tends to be a big challenge for circuit simulators. Applying time domain techniques to compute the oscillator steady states can be difficult because of long simulation times (especially for high-Q oscillators) and the stringent error tolerances usually necessary [1], [2].

The well-known frequency-domain technique harmonic balance (HB) [1], [3], [4] can be applied to compute the periodic steady state (PSS) of an oscillator, by considering the unknown frequency of oscillation to be an additional variable [1]. By restricting the phase of one harmonic of any circuit waveform, a square system of equations is obtained, which can be solved in principle for a unique solution. However, nonlinear solution of these equations is usually very challenging. That the DC solution is also a (trivial) steady state solution contributes to the challenge, as does the fact even relatively small deviations in the frequency during the HB Newton-Raphson tend to drive the circuit waveform estimates away from the solution, and vice-versa. A very good initial guess of the solution is usually required for oscillator steady-state methods to succeed.

In recent years, several methods have been developed to overcome the problem of computing the PSS of an oscillator. Techniques have been proposed to improve the convergence of harmonic balance when applied to oscillator circuits [5], [6]; in particular, the fruitful concept of *probes* has been proposed and applied [7]. A probe is a sinusoidal voltage source that acts as an external stimulus to the oscillator, usually at an estimated frequency close to the oscillator's natural frequency. Attaching a probe to an oscillator is intended to convert the circuit from an autonomous one (where the frequency is unknown) to a driven one (with frequency equal to that of the probe). (Although not explicitly mentioned in the prior literature on probe methods, the concept relies fundamentally on the phenomenon of injection locking [8].) Without the frequency as an unknown, the (locked) oscillator tends to converge much more easily to its driven steady state.

Since the intent is to eventually find the oscillator's natural frequency, the probe's frequency and amplitude are varied in a systematic manner to reach values where, in principle, the probe voltage source feeds no current at all into the oscillator. In other words, the probe waveform should exactly match that of the unprobed oscillator at the node the probe is connected to, with the result that it can be disconnected without affecting the solution of the circuit. Changing the probe's amplitude and frequency is achieved using a small set of extra ("upper level") equations that contain these two variables as unknowns. The equations set the amplitude and phase of the probe source's current to zero, *i.e.*, enforcing disconnection of the probe at solution. A small "upper-level Newton-Raphson" system is run in the upper-level equations; each iteration of this system involves evaluating the probe current, which is achieved by solving the driven oscillator's HB equations (the "lower-level Newton"). The probe technique thus decomposes the problem into two separate nonlinear problems, solved hierarchically.

Although probe methods have succeeding in improving oscillator steady-state convergence, convergence of the upper Newton has itself posed problems. Further, removal of the probe, even after success of the upper-level Newton, can lead to non-convergence of the un-probed oscillator initialized by the probe method's solution. Prior attempts to alleviate these problems include the application of continuation and homotopy methods [9]–[11] to the upper level Newton [12], [13].

In this paper, we identify an important mechanism why existing sinusoidal probe methods do not completely realize the full potential of the probe concept, and propose a simple remedy. The fallacy of existing probe methods is in assuming that a purely sinusoidal probe is capable of exactly matching the voltage waveform at the point of attachment to the oscillator. Given that amplitude stability of oscillators is critically dependent on nonlinear elements, oscillator waveforms in general contain not only first harmonic components, but also DC and higher harmonic components. For the probe voltage source to truly replicate the oscillator's waveform at its point of connection, it needs to track and find these other components also. In our simple extension of the probe method (termed the Multi-Harmonic Probe method, or MHP), we use a probe with using N harmonic components, where N is the number of harmonics that the lower-level oscillator HB equations consider. The upper-level probe equations now increase in size to N extra equations and unknowns.

Advantages of MHP over the standard probe techniques include improved convergence properties, an exact guarantee (within numerical representation limitations) that MHP's solution does represent the solution of the unprobed oscillator. The general applicability of MHP to any oscillator, especially ones with significant harmonic content like ring and relaxation oscillators, is another significant benefit from an implementation and deployment viewpoint, since a single technique can now be used for robust oscillator steady-state solution rather than specialized techniques (*e.g.*, for ring oscillators [14]).

The remainder of the paper is organized as follows. In section II, we review the standard probe method and discuss its limitations. In section III, we present the MHP technique, which generalizes existing sinusoidal probe techniques to arbitrary periodic probes. The Jacobian needed to solve the upper-level non-linear MHP equations is presented in the Appendix. In section IV, the MHP technique is applied to two LC oscillators and a ring oscillator.

II. Review of the standard probe technique

The standard circuit probe technique was apparently first proposed by Ngoya et al [7] and then extended by Gourary [12]. The probe, which acts as an external stimulus to the oscillator circuit, relies on the phenomenon of *injection locking*, converting the autonomous circuit into a non-autonomous circuit whose frequency equals the injection frequency of the stimulus (probe) [8], [15]. It should be noted that the range of frequencies of the probe is limited to ensure that the oscillator indeed does become injection locked. This plays a crucial rôle especially for high-Q crystal oscillators, where this range can be very limited.

The probe method essentially casts the problem as two conceptually independent sets of equations ("levels"). In the upper level, the

0-7803-9254-X/05/$20.00 ©2005 IEEE.

set of nonlinear equations to be solved is

$$\Re(I_{probe}(V_{probe},\omega)=0, \quad (1)$$

$$\Im(I_{probe}(V_{probe},\omega)=0, \quad (2)$$

where I_{probe} and V_{probe} represent the value of the fundamental harmonics of the probe current and voltage respectively. To select one from the infinite continuum of arbitrarily phase-shifted solutions, the phase of V_{probe} can be fixed to a particular value. The probe current is calculated at the "lower level", where the probe voltage and frequency are fixed, using the standard harmonic balance technique.

Prior probe techniques have employed purely sinusoidal probes [12]–[14]. However, the fundamental requirement, that the probe becomes electrically isolated after (1) and (2) are satisfied, is not generally true for purely sinusoidal probes. Because the probed node of an oscillator may not feature purely sinusoidal waveforms, DC and higher harmonic probe current components can persist even if (1) and (2) are satisfied, hence the probe is not truly isolated.

III. The Multi-harmonic Probe Technique

To remedy this situation, we propose the use of probes that feature not only a fundamental harmonic component, but also all other harmonic components. In our multi-harmonic probe (MHP) method, a *non-sinusoidal periodic probe* is employed. Consideration of all harmonics ensures that when the appropriate upper-level equations are solved, the probe is truly isolated from the oscillator, with the solution equalling the original oscillator's unprobed solution.

We now sketch the derivation of the MHP equations. The circuit equations of an oscillator (without any probe) can be represented in DAE form as

$$\frac{d}{dt}q(x(t))+f(x(t))+b=0, \quad (3)$$

where $x(t)$ is the vector of unknowns (of size n) to be solved for, n being the number of circuit waveforms (branch currents and node voltages). b is a vector of constant voltage/current sources.

When a voltage probe is added to the circuit, the above DAE is augmented by its equations to become

$$\frac{d}{dt}q_a(y(t))+f_a(y(t))+\begin{bmatrix}b\\0\end{bmatrix}-e_{n+1}v_{probe}(t)=0, \quad (4)$$

where

$$y(t)=\begin{bmatrix}x(t)\\ i_{probe}(t)\end{bmatrix}, \quad (5)$$

$$f_a(t)=\begin{bmatrix}f(t)\\0\end{bmatrix}+\begin{bmatrix}-i_{probe}(t)\\ \vdots \\ x_1(t)+R_{pr}i_{probe}(t)\end{bmatrix}, \quad (6)$$

$$q_a(t)=\begin{bmatrix}q(t)\\0\end{bmatrix}, \quad (7)$$

and R_{pr} is (optionally) a small resistor connected between the MHP and the oscillator. The purpose of the resistor is to limit current excursions during intermediate Newton steps at the upper and lower levels. $y(t)$, $f_a(t)$ and $q_a(t)$ are all vectors of length (n+1).

Using (5), we can obtain the MHP current from the unknowns of the oscillator-MHP circuit as

$$i_{probe}(t;\mathbb{V},\omega)=e_{n+1}^T y(t;\mathbb{V},\omega), \quad (8)$$

where $\mathbb{V}$, ω represent the Fourier coefficients and the frequency of a periodic $v_{probe}(t)$.

Analogous to the standard probe approach [12], MHP essentially casts the problem into two conceptually independent sets of equations ("levels"). At the lower level, standard (non-oscillatory) harmonic balance is used to to obtain the Fourier coefficients of the MHP current, given a fixed MHP voltage and frequency from the upper level. The Fourier coefficients and frequency of the MHP are updated by applying Newton-Raphson to the upper level equations, which equate *all harmonics* of the probe current to zero. It should be noted that for each Newton iteration at the upper level, a Newton solution of the lower-level equations is completed. Once the upper level converges, thus isolating the oscillator from the MHP, the periodic steady state of the oscillator is obtained. In the following subsections, we state the equations to be solved at the lower and upper levels. (Detailed derivations are largely omitted, in the interest of brevity.)

A. Lower Level MHP Equations

The frequency domain representation of (4) can be expressed as

$$H_a(Y;\{V_i\}_{i=M}^{-M},\omega)=\omega\Omega_{basic}Q_a(Y)+F_a(Y)+S\begin{bmatrix}b\\0\end{bmatrix}-T\mathbb{V}=0, \quad (9)$$

where Y is a vector of Fourier coefficients of the unknowns in the oscillator-MHP circuit, S and T are sparse matrices of size (n+1)$N\times$ (n+1) and (n+1)$N\times N$ respectively, where the nonzero entries are

$$S(1+(i-1)N,i)= \quad 1 \quad \forall \quad 1\le i\le n+1 \quad (10)$$

and

$$T(nN+i,i)= \quad 1 \quad \forall \quad 1\le i\le N. \quad (11)$$

We term the vector of Fourier coefficients of $i_{probe}(t)$ as $\mathbb{I}$, which is obtained using (8) as

$$\mathbb{I}=PY. \quad (12)$$

P is a sparse matrix of size $N\times$ (n+1)N, whose nonzero entries are

$$P(i,nN+i)= \quad 1 \quad \forall \quad 1\le i\le N. \quad (13)$$

Using the system of nonlinear equations in (9), the following steps are used to obtain the Fourier coefficients $\mathbb{I}$:

1) Insert the given values of $\mathbb{V}$ and ω in (9).
2) Obtain the value of Y by solving the set of nonlinear equations (9) using the Newton-Raphson method.
3) Extract the Fourier coefficients of $i_{probe}(t)$ from Y using (12).

The above represent a mapping L, which generates output $\mathbb{I}$ when provided with inputs $\mathbb{V}$, ω. We express this as

$$\mathbb{I}=L(\mathbb{V},\omega). \quad (14)$$

Although it is, in general, difficult or impossible obtain any simple closed-form expression for $L(\cdot)$, note that evaluating $L(\cdot)$ simply corresponds to steps 2) and 3) above.

B. Upper Level MHP Equations

At the upper level of the MHP method, we solve for

$$\mathbb{I}=L(\mathbb{V},\omega)=0, \quad (15)$$

which is a set of N nonlinear equations in (N+1) variables, consisting of $\mathbb{V}$ which is a vector of size N; and ω, which is a scalar. We choose one particular solution of (15) by restricting the phase of one of the harmonics of $\mathbb{V}$. Without loss of generality, we fix the phase of the first harmonic of $\mathbb{V}$ using

$$\phi=aV_1-bV_{-1}=0, \quad (16)$$

where a and b are constants which are calculated from the initial guesses for V_1 and V_{-1} and are complex conjugates to each other. The above set of nonlinear equations in (N+1) variables can now be uniquely solved for $\mathbb{V}$ and ω. (Please refer to the Appendix for the computation of the Jacobian matrix needed to solve (15) and (16).)

IV. Numerical Results

In this section, we apply the MHP technique above to several oscillator examples: a Colpitts oscillator, a 3-stage ring oscillator and a crystal-based Pierce oscillator. For comparison purposes, the standard (single-harmonic) probe technique is also used to compute the PSS of these oscillators. As another baseline for comparison, transient analysis is performed on these oscillators. To further validate the MHP technique, we employ oscillator HB directly by providing known good initial guesses obtained from transient analysis. We show that the results match that of MHP exactly, demonstrating its validity and accuracy.

A. *Colpitts Oscillator*

The circuit of the Colpitts oscillator is shown in Fig. 1. The element values are: L=13.5nH, R_L=300Ω, R_1=1.753KΩ, R_2=2Ω, C_1=100fF, C_2=2pF, C_3=7.4pF, V_{dd}=6V and V_{ee}=-6V. The value of β of the BJT is 99. The MHP was connected to the collector of the BJT via a small resistor of value R_{pr}=10Ω as shown in Fig. 1. The oscillator waveform at the collector of the BJT was obtained using the inverse discrete Fourier transform and is shown in Fig. 2(a). The frequency is determined to be 1.16062GHz. The oscillator waveform at the collector of the BJT is shown in Fig. 2(b). The frequency is determined to be 1.23602GHz. The differences between Fig. 2(a) and Fig. 2(b) can be viewed by observing the absolute value of the Fourier coefficients (DC value is not shown) as shown in Fig. 3(a) and Fig. 3(b) respectively.

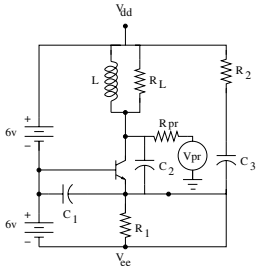

Fig. 1. Colpitts oscillator-MHP circuit.

The waveform at the collector of BJT in its steady state is plotted for one time period in Fig. 2(c), using transient analysis. This waveform exactly matches Fig. 2(a). The absolute values of the Fourier coefficients of this waveform are shown in Fig. 3(c), which exactly matches Fig. 3(a). The frequency was roughly estimated to be around 1.16GHz. We performed oscillator HB (as stated in section II) with good initial guess obtained from transient analysis. It should be noted that the oscillator HB indeed converges as the initial guess is very close to the solution. The frequency was determined to be 1.16062GHz which is exactly the same as calculated using MHP technique.

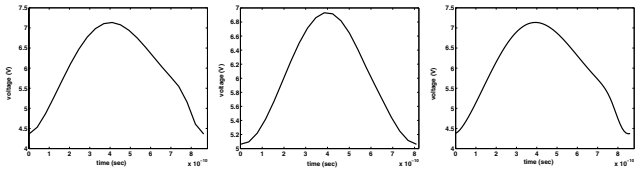

(a) MHP. (b) SP. (c) Transient.

Fig. 2. Time domain waveforms at the collector of BJT in the Colpitts oscillator in steady state.

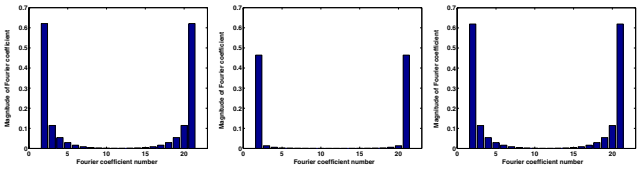

(a) MHP. (b) SP. (c) Transient.

Fig. 3. Magnitude of Fourier coefficients at the collector of BJT in the Colpitts oscillator in steady state.

B. *3 Stage Ring Oscillator*

The circuit of a 3-stage ring oscillator is shown in Fig. 4. The element values are: R_1=1KΩ, C_1=2pF. was used. The MHP was connected to the output (node A) via a small resistor of value R_{pr}=10Ω as shown in Fig. 4. The oscillator waveform at node A is shown in Fig. 5(a). The frequency is determined to be 153.50MHz. When a purely sinusoidal probe is connected to node A instead, the oscillator waveform at the output is shown in Fig. 5(b). The frequency is determined to be 149.103MHz. The differences in Fig. 5(a) and Fig. 5(b) can be seen by observing the absolute value of the Fourier coefficients of these two wave forms as shown in Fig. 6(a) and Fig. 6(b) respectively.

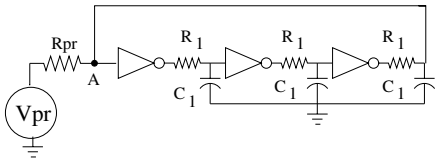

Fig. 4. 3 stage ring oscillator-MHP circuit.

The waveform at the output (node A) is plotted for one time period in Fig. 5(c), using transient analysis. This waveform exactly matches Fig. 5(a). The absolute value of Fourier coefficients of this waveform obtained by performing the discrete Fourier transform shown in Fig. 6(c) exactly matches Fig. 6(a). The frequency was roughly estimated to be around 153.50MHz. We performed oscillator HB with good initial guess provided from transient analysis. The frequency was solved by HB to be 153.50MHz, the same as calculated using the MHP technique.

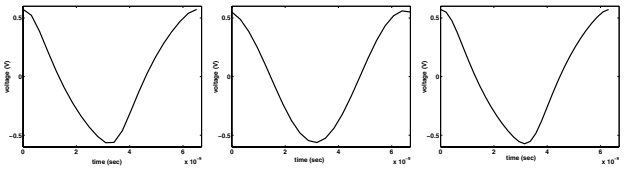

(a) MHP. (b) SP. (c) Transient.

Fig. 5. Time domain waveforms at the output of the 3 stage ring oscillator in steady state.

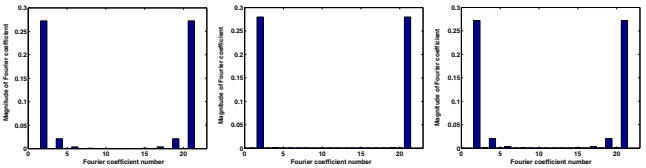

(a) MHP. (b) SP. (c) Transient.

Fig. 6. Magnitude of Fourier coefficients at the output of the 3 stage ring oscillator in steady state.

C. *Pierce Oscillator*

A Pierce oscillator circuit is shown in Fig. 7. The element values are: L_s=147nH, C_s=49.4fF, C_p=1.5pF, C_1=400fF, C_2=400fF, R_s=0.8, R_1=100KΩ, R_2=2.5KΩ. The value of β of the BJT is 99.

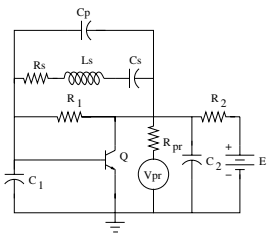

Fig. 7. Pierce oscillator-MHP circuit.

MHP was connected to the collector of the Pierce oscillator via a small resistor of value R_{pr} = 10Ω as shown in Fig. 7. The oscillator

waveform at the collector of the BJT is shown in Fig. 8(a). The magnitude of the Fourier coefficients of Fig. 8(a) is shown in 9(a). The frequency is determined to be 1.89491GHz. The crystal's Q factor is approximately $\frac{\omega L_s}{R_s}$ = 350.

A purely sinusoidal probe was also connected similarly and the upper level initialized with the solution obtained from the MHP technique. However, the purely sinusoidal probe simulation did not converge.

The oscillator waveform at the collector of BJT is plotted for one time period in Fig. 8(b), via transient analysis for over 10,000 cycles, with a time-step of 0.5e-9. This waveform matches that of Fig. 8(a). The absolute value of the Fourier coefficients of this waveform, shown in Fig. 9(b), matches Fig. 9(a). Oscillator HB, performed using a good initial guess obtained from transient analysis, also confirmed the MHP method's solution. The oscillator waveform, and the magnitude of its Fourier coefficients (shown in Fig. 8(c) and Fig. 9(c)) match Fig. 8(a) and Fig. 9(a), respectively. The frequency of oscillation was determined to be 1.89491GHz, the same as calculated using the MHP technique.

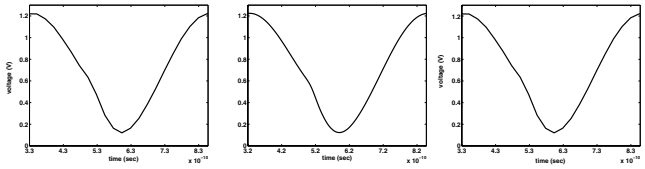

(a) MHP. (b) Transient. (c) Oscillator HB.

Fig. 8. Time domain waveforms at the collector of BJT in the Pierce oscillator in steady state.

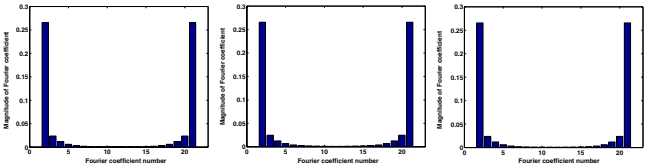

(a) MHP. (b) Transient. (c) Oscillator HB.

Fig. 9. Magnitude of Fourier coefficients at the collector of BJT in the Pierce oscillator in steady state.

V. Conclusion

A multi-harmonic extension to the standard single-harmonic probe technique for computing oscillator steady states has been presented. The new method uses non-sinusoidal periodic probes, enhancing the accuracy, convergence properties, and general applicability of probe methods. The method has been tested using LC, ring and crystal oscillator examples.

References

[1] J.K.White K.S.Kundert and A.Sangiovanni-Vincetelli. Steady State Methods for Simulating Analog Circuits and Microwave Circuits. Kluwer Academic Publishers, 1990.

[2] H.G.Brachtendorf and R.Laur. Transient simulation of oscillators. Technical Report ITD-98-34096K, Bell Laboratories, 1998.

[3] R.J.Gilmore and M.B.Steer. Nonlinear circuit analysis using the method of harmonic balance - a review of the art. International Journal of Microwave and Millimeter Wave Computer- Aided Engineering, 1(4):159–180, April 1991.

[4] K.S. Kundert and A. Sangiovanni-Vincentelli. Simulation of nonlinear circuits in the frequency domain. IEEE Trans. Computer-Aided Design, 5:521–535, October 1986.

[5] A.Costanza V.Rizzoli and A.Neri. Harmonic balance analysis of microwave oscillators with automatic suppression of degenerate solutions. Electronics letters, 28(3):256–257, January 1992.

[6] C.R.Chang, M.B.Steer, S.Martin, and Jr.E.Reese. Computer-aided analysis of free running microwave oscillators. IEEE Transactions on Microwave Theory and Techniques, 39(10):1735–1745, October 1991.

[7] E.Ngoya, A.Suarez, R.Sommet, and R.Quere. Steady State analysis of free or forced oscillators by harmonic balance and stability investigation for periodic or quasiperiodic regimes. International Journal of Microwave and Millimeter wave Computer- Aided Engineering, 5(3):210–233, March 1995.

[8] R. Adler. A study of locking phenomena in oscillators. Proceedings of the I.R.E. and Waves and Electrons, 34:351–357, June 1946.

[9] E.L.Allgower and K.Georg. Numerical Continuation Methods. Springer-Verlag, New York, 1990.

[10] J.Roychowdhury and R.C.Melville. Homotopy Techniques for Obtaining a DC Solution of Large-Scale MOS Circuits. In DAC, June 1996.

[11] L.T.Watson, S.C.Billups and A.P.Morgan. Algorithm 652: HOMPACK: a suite of codes for globally convergent homotopy algorithms. ACM Trans. Math. Software, 13:281–310, 1987.

[12] M.Gourary, S.Ulyanov, M.Zharov, S.Rusakov, K.K. Gullapalli, and B. J. Mulvaney. Simulation of High-Q Oscillators. IEEE/ACM international conference on Computer-aided design, pages 162–169, November 1998.

[13] Xiaochun Duan and Kartikeya Mayaram. Frequency Domain Simulation of High-Q Oscillators with Homotopy Methods. ICCAD, 2004.

[14] X.Duan, Y.Hu, and K.Mayaram. Simulation of Ring Oscillators using the Harmonic Balance Method. Proc. NEWCAS, 2004.

[15] K. Kurokawa. Injection locking of microwave solid state oscillators. Proc. IEEE, 61:1386–1410, October 1973.

Appendix

A. MHP upper level Jacobian

We term the Jacobian needed to solve (15) and (16) as J_{upper}, where

$$J_{upper} = \begin{bmatrix} \frac{\partial \mathbb{I}}{\partial \mathbb{V}}, \frac{\partial \mathbb{I}}{\partial \omega} \\ \frac{\partial \phi}{\partial \mathbb{V}}, \frac{\partial \phi}{\partial \omega} \end{bmatrix}. \tag{17}$$

From (17) it is clear that to compute J_{upper} we need to evaluate $\frac{\partial \mathbb{I}}{\partial \mathbb{V}}$, $\frac{\partial \mathbb{I}}{\partial \omega}$, $\frac{\partial \phi}{\partial \mathbb{V}}$ and $\frac{\partial \phi}{\partial \omega}$.

1) **Evaluation of $\frac{\partial \mathbb{I}}{\partial \mathbb{V}}$**

a) Differentiating (9) w.r.t to $\mathbb{V}$, we have

$$\omega \Omega_{basic} \frac{\partial Q_a(Y)}{\partial Y} \frac{\partial Y}{\partial \mathbb{V}} + \frac{\partial F_a}{\partial Y} \frac{\partial Y}{\partial \mathbb{V}} - T = 0. \tag{18}$$

b) Differentiating (9) w.r.t to Y, we have

$$J_{low} = \omega \Omega_{basic} \frac{\partial Q_a(Y)}{\partial Y} + \frac{\partial F_a(Y)}{\partial Y}, \tag{19}$$

where J_{low} is the Jacobian needed to solve the the set of nonlinear equations in (9).

c) Substituting (19) in (18) and rewriting explicitly in terms of $\frac{\partial Y}{\partial \mathbb{V}}$, we have

$$\frac{\partial Y}{\partial \mathbb{V}} = {J_{low}}^{-1} T. \tag{20}$$

d) Differentiating (12) w.r.t to $\mathbb{V}$ and substituting (20) ,we obtain

$$\frac{\partial \mathbb{I}}{\partial \mathbb{V}} = P {J_{low}}^{-1} T. \tag{21}$$

2) **Evaluation of $\frac{\partial \mathbb{I}}{\partial \omega}$**

a) Substituting (19) in the equation obtained by differentiating (9) w.r.t to ω and rewriting explicitly in terms of $\frac{\partial Y}{\partial \omega}$, we have

$$\frac{\partial Y}{\partial \omega} = -{J_{low}}^{-1} \Omega_{basic} Q_a(Y). \tag{22}$$

b) Differentiating (12) w.r.t to ω and substituting (22), we obtain

$$\frac{\partial \mathbb{I}}{\partial \omega} = -P {J_{low}}^{-1} \Omega_{basic} Q_a(Y). \tag{23}$$

3) **Evaluation of $\frac{\partial \phi}{\partial \mathbb{V}}$ and $\frac{\partial \phi}{\partial \omega}$**

a) Differentiating (16) w.r.t to $\mathbb{V}$, we have

$$\frac{\partial \phi}{\partial \mathbb{V}} = [0 \quad a \quad 0 \quad \dots \quad 0 \quad -b], \tag{24}$$

where $\frac{\partial \phi}{\partial \mathbb{V}}$ is a row vector of size N.

b) Differentiating (16) w.r.t to ω, we have

$$\frac{\partial \phi}{\partial \omega} = [0]. \tag{25}$$